

Review on non-conventional machining of shape memory alloys

M. MANJIAH¹, S. NARENDRANATH¹, S. BASAVARAJAPPA²

1. Department of Mechanical Engineering, National Institute of Technology, Surathkal, Karnataka, India;

2. Department of Studies in Mechanical Engineering, University B.D.T. College of Engineering,
Davangere 577004, Karnataka, India

Received 19 April 2013; accepted 22 September 2013

Abstract: Shape memory alloys (SMAs) are the developing advanced materials due to their versatile specific properties such as pseudoelasticity, shape memory effect (SME), biocompatibility, high specific strength, high corrosion resistance, high wear resistance and high anti-fatigue property. Therefore, the SMAs are used in many applications such as aerospace, medical and automobile. However, the conventional machining of SMAs causes serious tool wear, time consuming and less dimensional deformity due to severe strain hardening and pseudoelasticity. These materials can be machined using non-conventional methods such as laser machining, water jet machining (WJM) and electrochemical machining (ECM), but these processes are limited to complexity and mechanical properties of the component. Electrical discharge machining (EDM) and wire EDM (WEDM) show high capability to machine SMAs of complex shapes with precise dimensions. The aim of this work is to present the consolidated references on the machining of SMAs using EDM and WEDM and subsequently identify the research gaps. In support to these research gaps, this work has also evolved the future research directions.

Key words: non-conventional machining; electrical discharge machining; wire EDM; shape memory alloys

1 Introduction

In recent years, the materials such as titanium–nickel based shape memory alloys (SMAs) and other SMAs are commonly used in medical and industrial engineering applications. The medical applications include eyeglass frames, surgical stents, orthodontic arch wires, active catheters. The industrial engineering applications are functional devices such as fasteners, sealing and coupling, aerospace actuators (magnetic), sensors and microelectromechanical systems (MEMS), cellular phone antennas, fuel injector and small helicopter rotor [1]. Recently, TiNi alloys have been developed for many applications in MEMS due to their recovery strain and recovery force [2–4]. SMAs exhibit excellent properties such as quick actuation response, unique properties like superplasticity, shape memory effect (SME), high wear resistance, high corrosion resistance, great ductility, high specific strength and modulus, good fatigue property and high bio-compatibility [5,6]. These alloys are known for their SME and pseudoelasticity (PE). Among SMAs, TiNi based, Cu and Fe based SMAs

are widely accepted in industries [6,7].

The TiNi SMAs exhibit more than 8% recoverable strain compared to other SMAs. Many investigations have been made to study the effect of ternary alloying elements, such as Mo, Al, Hf, Co, Pt, Au, Cr, Cu, Nb, and Zr on phase transformation behaviour, SME and superelasticity. They are expected to operate at higher frequencies and temperature. The addition of Cu in TiNi SMAs increases the ductility and enhances the machinability characteristics, thereby reduces the liquidus temperature. This also decreases the hysteresis and detwinning stress of the martensite [4,5]. The addition of Zr reduces liquidus temperature and increases the transformation temperature to 200 °C [8]. Cu based SMAs have strengthened parent phase due to the refinement of grain size. It limits the size of martensite twins, thus decreasing the martensitic transformation temperature [9]. Hafnium based TiNi SMAs are potentially high temperature operating alloys up to 225 °C [10]. The developing of these SMAs in several sectors requires desired components for the particular operation hence the machining of these alloys is essential.

2 Conventional machining of SMAs

The SMA applications in manufacturing industries or medical sector require accurate dimensions and tolerances with optimal machining capabilities at lower production cost. Hence demand of the manufacturing for micro-devices of SMAs for such applications is increasing relatively. Manufacturing of complex SMA devices requires high precision and accurate machines. The machining can be performed by conventional and also by advanced machining methods. LIN et al [6], WEINTERT and PETZOLDT [11] and WU et al [12] have made an attempt to understand the conventional machining characteristics of TiNi SMAs. The special properties of SMAs lead to difficulty in machining, because of the presence of intermetallic compounds, strain hardening effect, cyclic hardening and fragments of alloy adhered on the surface of the tool. The time required for operation, depressing in cutting ability, higher tool wear, hardening of the machined surface and poor surface finish are the other causes, which further limits the conventional machining of SMAs.

In past few decades, SMAs are gaining wide scope in many engineering applications. The industries of electronic, medical, automobile and aerospace are demanding miniaturization in the devices with high accuracy and cost effectiveness [13]. However, the conventional machining of SMAs is associated with difficulties such as high operating temperature, less accurate and high cost. Hence, the non-conventional machining is an endless evolving technique to manufacture microscale SMA devices with desired accuracy. The machining of SMAs is challenging task and demands further development, hence it finds scope to study in detail about machinability of SMAs. Thus this work will focus on the machinability aspects of TiNi based SMAs. The non-conventional machining was considered for the current references. During the survey, the machinability aspects of SMAs contributed by earlier researchers have been presented and discussed extensively.

3 Non-conventional machining of SMAs

To overcome machining difficulties, some of the non-conventional techniques, such as laser machining, electric discharge machining (EDM), wire-EDM (WEDM), hybrid machining and so on, have been developed to machine the SMAs. However, special machining methods have their own limitations [6,7, 14].

Laser machining and EDM are widely used for machining of SMAs. In laser machining, less thermal and electrically conductive materials are used. In spite of this during laser cutting, the surface alteration of

machined zone and formation of residual zone must undergone further removal process [15]. Electrically conductive materials of any hardness can be machined easily and effectively using EDM. EDM is substitute process of laser machining for machining of complex and intricate shapes [16]. WEDM is electro-thermal process and has ability to machine precisely 3D regular and irregular structures. Micro parts with high degree of accuracy can be anticipated with lower residual stresses and better surface finish [17]. During finishing operation, energy generated per pulse is relatively lesser, and relatively less change in mechanical properties is caused due to low residual stresses, hence better surface finish can be achieved.

3.1 Laser machining

LI et al [18] investigated the machining of TiNi SMA using femtosecond laser. They explored the tool path and technique to manufacture precise components. The femto-second laser machining is basically thermal mechanism which causes high ablation rate and significant recast layer, the lower beam influences higher cutting quality and low cost. High quality, recast free and precise components can be obtained using optimal sideways movement in high laser. TUNG et al [19,20] presented SMA actuator using laser machining for medical applications. They reported that the mechanical properties will be improved, but the characteristic property of SMA such as large hysteresis is challenging. The geometry and dimensions are controlled by the tolerances of the laser machining and electropolishing.

3.2 Electrochemical polishing

LEE and SHIN [21] studied the electrochemical polishing of TiNi SMA with parameters such as electrolyte composition, applied current, machining time and inter electrode gap, and analyzed the machined surface. The neutral electrolyte removed material at faster rate, but caused innumerable ultramicroholes on the surface compared to acidic electrolyte. The acidic electrolyte has less material removal rate and lower ultra micro hole on the machined surface. The better surface roughness can be achieved by higher current and smaller inter electrode gap. LEE et al [22] analysed the experimental and simulation results of electrochemical machining on TiNi SMA. The simulated results were different from the experimental data due to different power sources used in simulation, the MRR increases with the current density and duty factor. The high current yields poor surface quality, and duty factor influences the electrochemical reaction.

3.3 Water jet machining

KONG et al [7] reported the plain and abrasive

water jet machining characteristics of TiNi SMA. The study revealed that, abrasive water jet (AWJ) machining has better depth control in milling operation than plain water jet (PWJ) machining of TiNi SMA. AWJ machining has greater thermal effect than PWJ machining due to high impact velocity of abrasive particles. The concise area collision by abrasive particle of high velocity can reach a temperature superior than the austenite transformation, it will cause the melting of material. This may involve the phase change of NiTi from martensite to austenite. The cracks are initiated and propagation may start in Ti₂Ni region rather than TiNi. They suggested that the AWJ machining could be an effective and efficient way for machining of TiNi SMA which possesses a complexity in crystal structure and phase transformation.

FROTSCHER et al [23] conducted experiment on machining of TiNi sheets. The machined performance aspects are compared between the WJM and micro-milling. The WJM is favorable with respect to cutting time, thermal influence of workpiece and machining costs compared to micro-milling. However, the burr remains in the machining and de-burring is required.

3.4 EDM of SMAs

In EDM, discharge sparks are utilized to melt and evaporate the material. The dielectric fluid is used as a medium between the electrode and workpiece. The highly complex shapes can be machined using EDM with high precision.

3.4.1 MRR in EDM

Material removal rate (MRR) is one of the significant factor influences the machinability of materials. CHEN et al [16] investigated the electric discharge machining characteristics of a NiAlFe shape memory alloy. The machining properties were evaluated as a function of MRR, electrode wear ratio (EWR), surface roughness and cross sectional surface topography of machined surface. The MRR of NiAlFe ternary shape memory alloy significantly relates to the discharge energy and grows with the increase in discharge current. The MRR is generally dependent on melting temperature and thermal conductivity of SMAs. Higher melting temperature of the material yields less melting and evaporation. The higher thermal conductivity of material causes more energy transfer to the nearby matrix leading to lower MRR. The higher peak current has higher current density, which leads to more melting of material, evaporation and increases the impact force of dielectric fluid. The MRR is also affected by pulse on time. At higher pulse on time, melting and evaporation of material are more due to accumulated discharge energy causing greater MRR [24].

The MRR depends on the optimum pulse on time, current and combination of energy transmit per pulse frequency. The longer pulse on time reduces the energy density of discharge spark caused by the expansion of plasma channel. The molten material cannot flow away from the machined surface effectively due to insufficient plasma energy to explode the dielectric fluid. Hence, the MRR decreases with the increase in pulse duration [25]. The MRR is lesser at shorter pulse duration because of less vaporization of material. This may also be similar in machining of other materials. The MRR is high in rotary electrode compared to stationary due to the fact that the debris removal is superior and effective from the machined surface caused by the centrifugal force of rotating electrode. The electrode polarity also plays a significant role in MRR. The positive polarity has higher MRR due to more transfer of energy. The EWR is also similar to the MRR. The positive polarity electrode shows higher wear rate along with higher MRR. The dielectric fluid concentration and additive may also affect the MRR and EWR [26,27]. The EWR increases with the increase in pulse on time at various peak currents and decreases when it reaches optimum value. This is also dependent on the material property and discharge energy [28,29].

3.4.2 Surface and subsurface quality of SMAs

The machined surface roughness increases with the increase in the peak current and pulse on time. The higher current produces discharge energy sparks which strikes on the surface strongly, resulting in more amount of erosion of material and higher surface roughness. The material with low melting temperature and thermal conductivity exhibits higher surface roughness [16]. The larger pulse on time generates larger discharge energy to melt and evaporate the material. The deeper crater will form on the machined surface, which leads to higher surface roughness. The surface roughness of EDM is also dependent on the material melting temperature and thermal conductivity [25].

The machining of TiNi components significantly depends on the machining conditions. The higher cutting conditions improve the workpiece quality, but causes the changes in the subsurface due to the higher heat generation. The machined surface generally consists of recast layer, white layer, oxides, contaminants from the tool and the heat affected zone. This may result in increased microhardness in the subsurface of the component. The increase in the hardness at the outer surface is arising from the severe strain hardening and fatigue hardening effect. Figure 1 shows the hardness of surface of TiNiZr, TiNiCr and NiAlFe SMAs machined using EDM. It indicates that the hardness of the specimen near the outer machined surface can reach high hardness value. The hardness remains the same at depth

greater than 100 μm below the machined surface which is the bulk hardness of the material. The higher hardness near the machined surface is due to the formation of Cr_2O_3 , ZrO_2 , TiO_2 , TiNO_3 , TiC , Fe_2O_3 , Al_2O_3 and NiO and the deposition of particles on the recast layered surface [16,25,29].

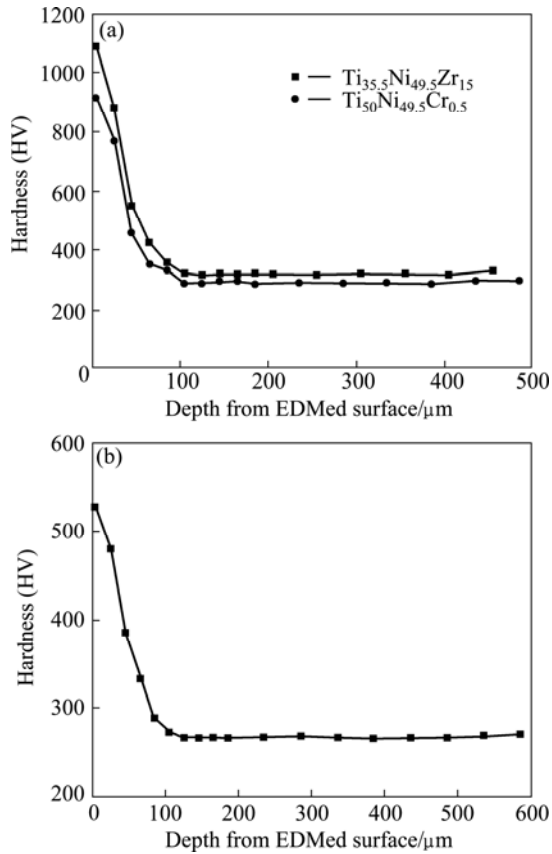


Fig. 1 Hardness at various distances from EDMed surface of SMAs: (a) TiNiZr and TiNiCr [25]; (b) NiAlFe [16]

Figure 2 shows the SEM micrographs of EDMed NiAlFe and TiNiZr ternary SMA. It clearly depicts that the formed melting drops and larger recast layer deposited on the machined surface at higher peak current and pulse on time. In Fig. 2(b), the circle shows the electro discharged crater formed on the machined surface during EDM. The surface contains several oxides and compounds formed during the electric discharge machining. The white arrows in Fig. 2(a) show the recast layer deposited on the surface, and the black arrows in Fig. 2(b) shows the oxide layers which contain Fe_2O_3 , Al_2O_3 , NiO , C , Cu_2O , TiNO_3 , ZrO_2 and Ni rich region [16,25,29].

Figure 3 shows the cross sectional micrographs of the EDMed NiAlFe SMA surface at various pulse on time. The recast layer thickness was observed clearly for various pulse on time containing several oxides and compounds. Initially increased recast layer thickness is observed from the cross sectional image. The flow ratio of positive ions in the plasma channel increases with

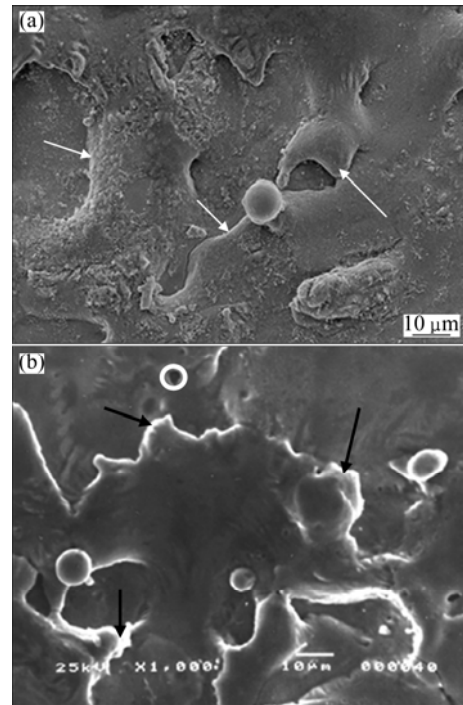


Fig. 2 SEM micrographs of EDMed surface for NiAlFe alloy [16] (a) and TiNiZr alloy [25] (b)

pulse duration. The reduced recast layer thickness was observed in the 25 μs of pulse on time, meanwhile the higher MRR, due to the high discharge energy pressurizes the dielectric fluid, it helps to push out the molten material and debris from the machined surface. At further extended pulse on time to greater than 25 μs , drastic increase of recast layer thickness was noticed. It is primarily because higher accumulated discharge energy melts relatively larger amount of material and recast on the machined surface. The melted material didn't move away from the surface, hence the thickness of the recast layer increased [16,25].

3.5 WEDM of SMAs

3.5.1 MRR in WEDM

The WEDM is a type of EDM where the material is eroded from the surface using the number of sparks generated by the wire. HSIEH et al [30] studied the machining characteristics and shape recovery ability of TiNiZr/Cr SMAs using WEDM. In WEDM, material erosion takes place by series of discrete sparks. The feed rate of wire electrode increases with increase in pulse on time. The discharge energy grows with the increase of pulse on time, resulting in higher MRR. In WEDM, MRR is associated with melting temperature and thermal conductivity of material. However, WEDM doesn't depend on the mechanical properties and crystal structure of the materials. Hence, this can be used to estimate the machining characteristics of ternary SMAs using WEDM.

3.5.2 Surface and subsurface quality of SMAs

The surface roughness increases with the growing pulse duration. The surface roughness is connected with the number of craters distribution on the machined surface during the spark discharge [31]. The surface roughness of SMAs increases with increase in pulse on time and peak current. The surface quality also depends on the wire material, dielectric fluid, flushing pressure and the amount of transferred materials on the machined surface [31]. The longer pulse on time forms larger and deeper craters exhibiting greater surface roughness. The surface roughness is also associated with the material melting temperature and thermal conductivity of SMAs. The lower thermal conductivity and melting temperature has higher surface roughness. The extended pulses

discharge more energy to melt and evaporate, and they penetrate into larger depth causing bigger crater. Apart from the surface craters, the cracks are formed in the melting zones and generated between the crater and the colder surroundings [32,33].

The residual stresses and crack density are arisen by the plastic deformation or phase transformation in the material, and the penetration depth of residual stress is limited. The deformed layer hardness is higher than the bulk material hardness. Thermally affected layer that is white layer and recast layer in the machined surface because of the high temperature is obtained by the spark. The changes in the machined surface are mainly affected by temperature effect and high cooling rate. Figure 4 shows the cross sectional hardness of the WEDMed

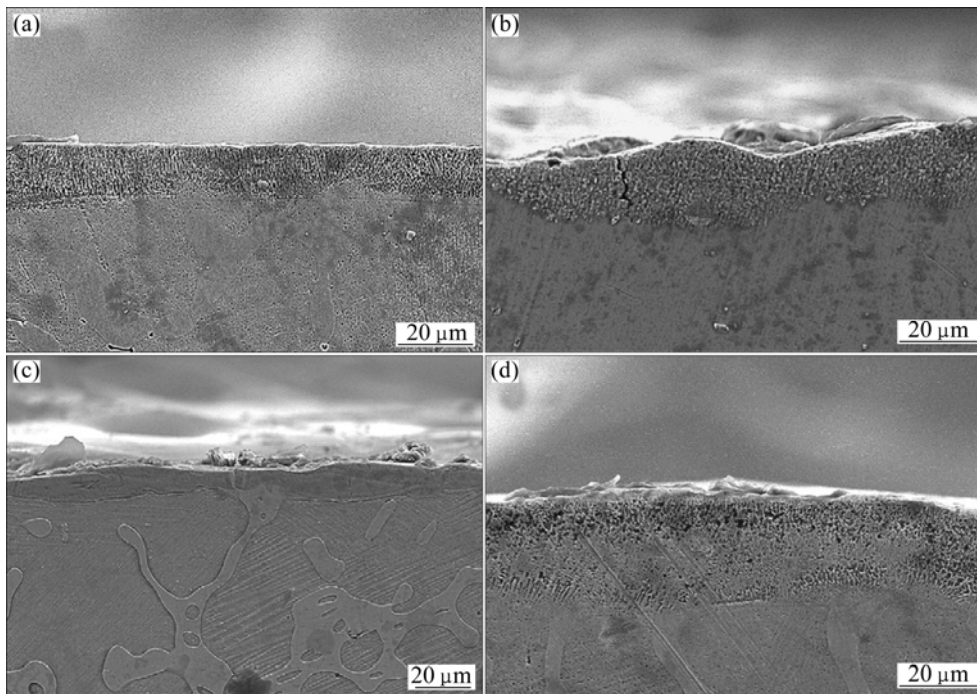


Fig. 3 Cross-sectional micrographs of surface layer machined using EDM for NiAlFe SMA at peak current of 10 A and pulse on time of 6 μs (a), 12 μs (b), 25 μs (c), and 100 μs (d) [16]

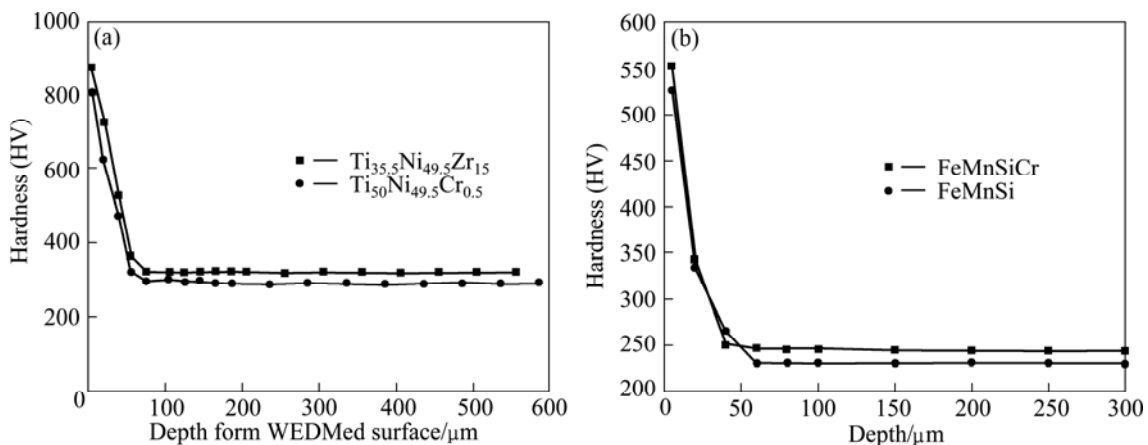


Fig. 4 Hardness at various distances from surface of SMAs machined using WEDM: (a) TiNiZr and TiNiCr [30]; (b) FeMnSiCr and FeMnSi [33]

surface of TiNiZr, TiNiCr, FeMnSiCr and FeMnSi SMAs. The outer surface hardness is dependent on the recast layer thickness and it is higher than the bulk material hardness. It is because of the formation of oxides as discussed earlier during the EDM of surface and the hardening effect is noticed due to the formation of other compounds such as $\text{Cu}_{0.83}\text{Si}_{0.17}$, η' -(Cu, Si) (Fe, Cr) and TiC in the recast layer of the machined surface. They are mainly dependent on the machining parameters, dielectric fluid and the electrode material [28–33].

Figure 5 shows the melted recast layer of WEDMed surface on $\text{Ti}_{35.5}\text{Ni}_{49.5}\text{Zr}_{15}$ SMA. It is observed that craters, melted drops, cracks and the surface texture cause the roughness. This recast layer consists of some oxides as discussed in EDM surfaces of SMA. The recast layer also consists of Ni rich phases, TiO_2 , TiC and so on. The Cu_2O is formed on the machined surface due to the copper electrode [34,35]. The craters are formed on the machined surface, as shown in Fig. 5, which influences the surface roughness on the machining surface. The higher surface roughness appears probably because of higher discharge current and longer pulse on time which are influenced to form deeper and wider craters on the machined surface.

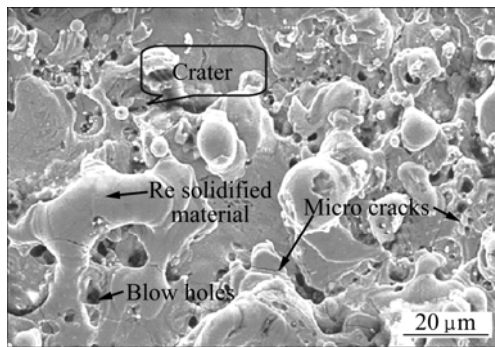


Fig. 5 Micrograph of surface machined using WEDM for $\text{Ti}_{35.5}\text{Ni}_{49.5}\text{Zr}_{15}$ alloy [30]

Figure 6 shows the thickness of recast layer formed on the machined surface. The recast layer can be reduced by higher pulse on time, because higher discharge energy impacts the dielectric fluid effectively which flushes away the molten material from the machined surface. The recast layer also influences the SME of the machined surface [29,30]. The thickness of recast layer affects the surface hardness because it contains different oxides, phases, compounds and matrix element. The recast layer thickness of SMA using WEDM can be controlled by choosing the optimum pulse on time, peak current and other process parameters.

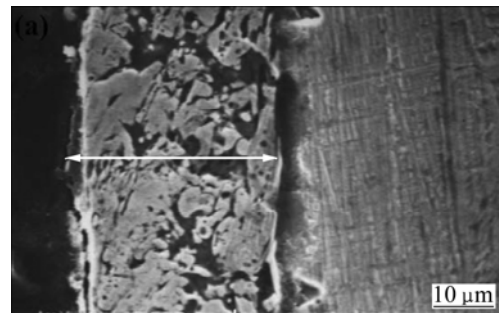


Fig. 6 Cross-sectional micrograph of Fe-30Mn-6Si alloy machined using WEDM [33]

4 Discussion

The consolidated contributions of the earlier researchers have been segregated and presented in Tables 1–3. Table 1 depicts the contribution of researchers on the SMAs machining using the EDM and WEDM. The authors have presented their investigation on the important aspects of machinability of SMAs. Very few researchers have worked on the machining of TiNi based SMAs. The machinability of SMAs is affected by the input parameters and other machining conditions.

Table 2 lists the parameters chosen and their levels on machining of SMAs. Few researchers mentioned the optimum parameters for achieving good responses. They

Table 1 Evaluation of EDM and WEDM on SMAs

No.	Authors	Process	Material	Brief contribution
1	CHEN et al [25]	EDM	TiNiCr and TiNiZr SMA	Investigated machining characteristics by hardness and surface roughness of machined alloys
2	CHEN et al [16]	EDM	NiAlFe and TiNiZr SMA	Studied machining characteristics
3	THEISEN and SCHUERMANN [32]	EDM	NiTi SMA	Determined surface modification in EDM
4	LIN et al [29]	EDM	TiNi and TiNiCu SMA	Studied the electro discharge machining characteristics of TiNi SMA
5	LIN et al [33]	WEDM	Fe-30Mn-6Si and Fe-30M-6Si-5Cr SMA	Observed crater and recast layer during WEDM
6	HSIEH et al [30]	WEDM	TiNiZr/Cr SMA	Studied machining characteristics and shape recovery ability of SMAs using WEDM

Table 2 Evaluation of nonconventional SMAs machining parameters

No.	Author	Process	Material	Parameter selected	Value	Optimum
1	CHEN et al [25]	EDM	TiNiCr and TiNiZr SMA	Discharge current, pulse duration, pause duration, gap voltage, dielectric	3–19 A, 3–100 μ s, 3–100 μ s, 50 V, kerosene	10 A, 12 μ s
2	CHEN et al [16]	EDM	NiAlFe and TiNiZr SMA	Discharge current, pulse duration, pause duration, gap voltage, dielectric	3–19 A, 3–100 μ s, 3–100 μ s, 50 V, kerosene	10 A, 25 μ s
3	THEISEN and SCHUERMAN [32]	EDM	NiTi SMA	Working voltage, working current, frequency, pulse duty factor, idle pulse	240 V, 2–4 kHz, 5%–20%, 80%, 40%	–
4	LIN et al [29]	EDM	TiNi and TiNiCu SMA	Pulse current, pulse duration, pause duration, gap voltage, electrode, dielectric	6–25 A, 3–100 μ s, 3–100 μ s, 50 V, copper, kerosene	12 A, 6–12 μ s
5	LIN et al [33]	WEDM	Fe–30Mn–6Si, Fe–30M–6Si–5Cr SMA	Pulse duration, pause duration, gap voltage, current, flushing	0.6 μ s, 11 μ s, 212 V, 1 A, 5 kg/cm ³	–
6	HSIEH et al [30]	WEDM	TiNiZr/Cr SMA	Pulse duration, pause duration, duty factor, gap voltage, current, flushing	1–5 μ s, 5 μ s, 0.6%, 50 V, 15 A, 5 kg/cm ³	–
7	LEE and SHIN [21]	EC polishing	NiTi SMA	Composition of electrolyte, pulse on/off time, current, inter electrode gap	A(H ₂ SO ₄ +H ₃ PO ₄ +H ₂ O), B(NaNO ₂ +Na ₂ C ₄ H ₄ O ₆), 800 μ s, 200 μ s, 3–18 A, 0.3–2 mm	Acidic electrolyte, 800 μ s, 200 μ s, 18 A, 0.5 mm
8	FROSTSCHER et al [23]	Water jet, micro milling	NiTi SMA	Mass flow rate, SOD	25 g/min, 2–8 mm	–
9	KONG et al [7]	WJM	NiTi SMA	Pump pressure, particle size, SOD, traverse rate	413.7 MPa, 180–300 μ m, 3 mm, 500–2000 mm/min	–

Table 3 Evaluation of nonconventional machined SMAs and applications

No.	Authors	Process	Material	Applications
1	CHEN et al [16]	EDM	NiAlFe and TiNiZr SMA	Limited to lower temperature
2	CHEN et al [25]	EDM	TiNiCr and TiNiZr SMA	Coupling and sealing
3	LIN et al [33]	WEDM	Fe–30Mn–6Si and Fe–30M–6Si–5Cr SMA	Coupling elements
4	LIN et al [29]	EDM	TiNi and TiNiCu SMA	Coupling and sealing
5	HSIEH et al [30]	WEDM	TiNiZr/Cr SMA	Coupling and sealing
6	LEE and SHIN [21]	ECM	NiTi SMA	Actuators and medical
7	FROSTSCHER et al [23]	WJM and micro milling	NiTi SMA	Actuators and medical
8	KONG et al [7]	WJM	NiTi SMA	Actuators and medical

have paid attention on the contributing electrical parameters such as pulse on time, pulse off time, discharge current, discharge voltage and non-electrical parameters such as type of dielectric fluid, flushing

pressure. The factors such as MRR, surface roughness and hardness were considered the output responses. A few research works have been reported on the effect of wire material (electrode), diameter of the wire, wire

tension, wire speed, concentration and additives of dielectric fluid, polarity of electrode and pulse wave form on the responses during WEDM of SMAs. The aspects of surface integrity were also considered in their research work.

It is observed from Table 4 that, the EDMed and WEDMed TiNi based alloys (considered SME thickness of 0.6 mm) exhibits perfect shape recovery at 3% strain and 5% bending strain but slightly reduction at 8% bending strain. Fe based SMA (considered SME thickness of 1 mm) exhibits a less shape recovery after WEDM at 2% and 4% bending strains. A NiAlFe alloy does not have shape recovery at 8% bending strain due to the presence of brittle β matrix phase. The authors conclude that the reduction in the shape recovery at higher bending strain is due to the effect of recast layer thickness. And if also have been lost due to precipitation of carbides and oxides formation in the melted zone.

Table 4 Shape memory property of alloys after machining [25,29,30,33,36]

Alloy	Shape recovery/%		
	$\varepsilon=3\%$	$\varepsilon=5\%$	$\varepsilon=8\%$
Ti ₅₀ Ni _{49.5} Cr _{0.5} (annealed)	100	100	90
Ti ₅₀ Ni _{49.5} Cr _{0.5} (EDMed)	100	99	83
Ti _{35.5} Ni _{49.5} Zr ₁₅ (annealed)	100	100	88
Ti _{35.5} Ni _{49.5} Zr ₁₅ (EDMed)	100	98	82
Ti ₅₀ Ni _{49.5} Cr _{0.5} (WEDMed)	100	99	85
Ti _{35.5} Ni _{49.5} Zr ₁₅ (WEDMed)	100	99	86
Ti _{35.5} Ni _{48.5} Zr ₁₆ (annealed)	100	97	90
Ti _{35.5} Ni _{48.5} Zr ₁₆ (EDMed)	96	91	80
Ni ₆₀ Al _{48.5} Fe _{15.5} (annealed)	42	35	–
Ni ₆₀ Al _{48.5} Fe _{15.5} (EDMed)	30	25	–

Alloy	Shape recovery/%		
	$\varepsilon=3\%$	$\varepsilon=6\%$	$\varepsilon=12\%$
Ti ₅₀ Ni ₅₀ (annealed)	100	100	86
Ti ₅₀ Ni ₅₀ (EDMed)	100	98	75
Ti ₄₉ Ni ₅₁ (annealed)	100	100	87
Ti ₄₉ Ni ₅₁ (EDMed)	100	99	75.5
Ti ₅₀ Ni ₄₀ Cu ₁₀ (annealed)	100	100	86.5
Ti ₅₀ Ni ₄₀ Cu ₁₀ (EDMed)	100	98	74

Alloy	Shape recovery/%	
	$\varepsilon=2\%$	$\varepsilon=4\%$
Fe–30Mn–6Si (annealed)	86.8	81.7
Fe–30Mn–6Si (WEDMed)	84.6	72.2
Fe–30Mn–6Si–5Cr (annealed)	93.7	88.2
Fe–30Mn–6Si–5Cr (WEDMed)	92.4	82.8

In previous references, Taguchi technique has been adopted to optimize and analyze the effect of process

parameters of EDM and WEDM on responses. However, other statistical techniques, such as 2^k factorial design of experiments, response surface methodology (RSM) and so on, are not adopted so far. It can also be noticed that there are no tools and techniques used for correlating input parameters with the responses. The advanced techniques, such as particle swarm optimization (PSO), advanced PSO, artificial neural network (ANN), genetic algorithm (GA), fuzzy logic (FL), computational system for the process design, artificial bee colony technique (ABC), tabu search, hybrid methods, mixed orthogonal array (OA), can be used to correlate experimental results and optimize process parameters. The thermal analysis can be done using FEM, and mathematical model can be developed to predict the responses. Modeling and simulation packages (Deform 3D) such as simulated annealing, cloud computing, teaching learning based optimization (TLBO) algorithm can be employed adequately to predict the responses.

Table 3 reveals the few applications of SMAs using EDM and WEDM. The TiNi based alloys have major applications in medical, micro actuator, coupling and sealing and MEMS. The production and machining of high temperature SMAs are also required for industrial and medical applications with better SME, pseudoelastic properties and superior mechanical properties.

5 Future trends

The references presented above reveal that the EDM and WEDM of SMAs have been reported on the pulse durations, discharge current and discharge voltage on the responses. Limited work has been reported on the TiNi based SMAs using WEDM and optimization of process parameters. There are inadequate data on the high temperature SMAs, other parameters affecting the responses, analysis of residual stresses generated in WEDMed surface and SME of WEDMed surface. Further study in this direction is needed to identify the effect of parameters on machining of SMAs, and in particularly more research focus is essentially on to the electrical and non electrical parameters such as pulse duration, peak current, discharge voltage, polarity, pulse wave form, dielectric fluid concentration, additives, wire material, wire diameter, wire tension, wire speed, and table feed on the machined surface. The analysis of SME, surface integrity and further manufacture of high temperature ternary SMAs is another open ended field in which research work can be carried out.

References

- [1] MING H W U, SCHETKY L M C D. Industrial applications for shape memory alloys [C]//Proceedings of the International

- Conference on Shape Memory and Superelastic Technologies. Pacific Grove, California, 2000: 171–182.
- [2] QIN Chang-jun, MA Pei-sun, YAO Qin. A prototype micro-wheeled-robot using sma actuator [J]. *Sensors and Actuators A: Physical*, 2004, 113: 94–99.
- [3] WINZEK B, SCHMITZ S, RUMPF H, STERZL T, HASSDORF R, THIENHAUS S, ET A L. Recent developments in shape memory thin film technology [J]. *Materials Science and Engineering A*, 2004, 378: 40–46.
- [4] THIENHAUS S, SAVAN A, LUDWIG A. Combinatorial fabrication and high-throughput characterization of a Ti–Ni–Cu shape memory thin film composition spread [J]. *Materials Science and Engineering A*, 2008, 482: 151–155.
- [5] ZHANG H J, QIU C J. A TiNiCu thin film micropump made by magnetron co-sputtered method [J]. *Materials Transactions*, 2006, 47: 532–535.
- [6] LIN H C, LIN K M, CHEN Y C. A study on the machining characteristics of TiNi shape memory alloys [J]. *Journal of Materials Processing Technology*, 2000, 105: 327–332.
- [7] KONG M C, AXINTE D, VOICE W. Challenges in using waterjet machining of NiTi shape memory alloys: An analysis of controlled-depth milling [J]. *Journal of Materials Processing Technology* 2011, 211: 959–971.
- [8] VERMAUT P, LITYŃSKA L, PORTIER R, OCHIN P, DUTKIEWICZ J. The microstructure of melt spun Ti–Ni–Cu–Zr shape memory alloys [J]. *Materials Chemistry and Physics*, 2003, 81: 380–382.
- [9] KANG S, LEE Y, LIM Y, NAM J, NAM T, KIM Y. Relationship between grain size and martensitic transformation start temperature in a Ti–30Ni–20Cu alloy ribbon [J]. *Scripta Materialia*, 2008, 59: 1186–1189.
- [10] FIRSTOV G S, VAN HUMBEECK J, KOVAL YU N. Comparison of high temperature shape memory behavior for ZrCu-based, Ti–Ni–Zr and Ti–Ni–Hf alloys [J]. *Scripta Materialia*, 2004, 50: 243–248.
- [11] WEINERT K, PETZOLDT V. Machining of NiTi based shape memory alloys [J]. *Materials Science Engineering A*, 2004, 378: 180–184.
- [12] WU S K, LIN H C, CHEN C C. A study on the machinability of a Ti_{49.6}Ni_{50.4} shape memory alloy [J]. *Materials Letter*, 1999, 40: 27–32.
- [13] BOYER R R. An overview on the use of titanium in the aerospace industry [J]. *Materials Science and Engineering A*, 1996, 213: 103–114.
- [14] ASKELAND D R, PHUE P P. The science and engineering of materials [M]. Gengage Learning, 2006.
- [15] CRACIUNESCU C M, MIRANDA R M, SILVA R J C, ASSUNC E, BRAZ FERNANDES F M. Laser beam interaction with Ni–Mn–Ga ferromagnetic shape memory alloys [J]. *Optics and Lasers in Engineering*, 2011, 49: 1289–1293.
- [16] CHEN S L, HSIEH S F, LIN H C, LIN M H, HUANG J S. Electrical discharge machining of a NiAlFe ternary shape memory alloy [J]. *Journal of Alloys and Compounds*, 2008, 464: 446–451.
- [17] HAN Fu-zhu, JIANG Jun, YU Ding-wen. Influence of discharge current on machined surfaces by thermo-analysis in finish cut of WEDM [J]. *International Journal of Machine Tools & Manufacture*, 2007, 47: 1187–1196.
- [18] LI C, NIKUMB S, WONG F. An optimal process of femtosecond laser cutting of NiTi shape memory alloy for fabrication of miniature devices [J]. 2006, 44: 1078–1087.
- [19] TUNG A T, PARK B, LIANG D H. Laser-machined shape memory alloy sensors for position feedback in active catheters [J]. *Sensors and Actuators A*, 2008, 147: 83–92.
- [20] TUNG A T, MEMBER S, PARK B, LIANG D H. Laser-machined shape memory alloy actuators for active catheters [J]. *ASME Transactions on Mechatronics*, 2007, 12: 439–446.
- [21] LEE E S, SHIN T H. An evaluation of the machinability of nitinol shape memory alloy by electrochemical polishing [J]. *Journal of Mechanical Science and Technology*, 2011, 25: 963–969.
- [22] LEE E, SHIN T, KIM B, BAEK S. Investigation of short pulse electrochemical machining for groove process on Ni–Ti shape memory alloy [J]. *International Journal of Precision Engineering and Manufacturing*, 2010, 11: 113–118.
- [23] FROTSCHER M, KAHLEYSS F, SIMON T, BIERMANN D, EGGELER G. Achieving small structures in thin NiTi sheets for medical applications with water jet and micro machining: A comparison [J]. *Journal of Materials Engineering and Performance*, 2011, 15: 776–782.
- [24] HADDAD M J, TEHRANI A F. Material removal rate (MRR) study in the cylindrical wire electrical discharge turning (CWEDT) process [J]. *Journal of Material Processing Technology*, 2007, 9: 369–378.
- [25] CHEN S L, HSIEH S F, LIN H C, LIN M H, HUANG J S. Electrical discharge machining of TiNiCr and TiNiZr ternary shape memory alloys [J]. *Materials Science and Engineering A*, 2007, 446: 486–492.
- [26] CHEN S L, YAN B H, HUANG F Y. Influence of kerosene and distilled water as dielectrics on the electric discharge machining characteristics of Ti–6Al–4V [J]. *Journal of Materials Processing Technology*, 1999, 87: 107–111.
- [27] LIN Y C, YAN B H, CHANG Y S. Machining characteristics of titanium alloy (Ti–6Al–4V) using a combination process of EDM with USM [J]. *Journal of Materials Processing Technology*, 2000, 104: 171–177.
- [28] HASCALIK A, CAYDAS U. Electrical discharge machining of titanium alloy (Ti–6Al–4V) [J]. *Applied Surface Science*, 2007, 253: 9007–9016.
- [29] LIN H C, LIN K M, CHENG I S. The electro-discharge machining characteristics of TiNi shape memory alloys [J]. *Journal of Materials Science*, 2001, 36: 399–404.
- [30] HSIEH S F, CHEN S L, LIN H C, LIN M H, CHIOU S Y. The machining characteristics and shape recovery ability of Ti–Ni–X (X=Zr, Cr) ternary shape memory alloys using the wire electro-discharge machining [J]. *International Journal of Machine Tools and Manufacture*, 2009, 49: 509–514.
- [31] JAHAN M P, RAHMAN M, WONG Y S. A review on the conventional and micro-electric discharge machining of tungsten carbide [J]. *International Journal of Machine Tool and Manufacture*, 2011, 51: 837–859.
- [32] THEISEN W, SCHUERMAN A. Electro discharge machining of nickel–titanium shape memory alloys [J]. *Materials Science and Engineering A*, 2004, 378: 200–204.
- [33] LIN H, LIN K, CHEN Y, CHU C. The wire electro-discharge machining characteristics of Fe–30Mn–6Si and Fe–30Mn–6Si–5Cr shape memory alloys [J]. *Journal of Materials Processing Technology*, 2005, 161: 435–439.
- [34] YILMAZ O, OKKA M A. Effect of single and multi-channel electrodes application on EDM fast hole drilling performance [J]. *International Journal Advanced Manufacturing Technology*, 2010, 51: 185–194.
- [35] KLOCKE F, WELLING D, DIECKMANN J. Comparison of grinding and Wire EDM concerning fatigue strength and surface integrity of machined Ti6Al4V components [J]. *Procedia Engineering*, 2011, 19: 184–189.
- [36] HSIEH S F, HSUE A W J, CHEN S L, LIN M H, OU K L, MAO P L. EDM surface characteristics and shape recovery ability of Ti_{35.5}Ni_{48.5}Zr₁₆ and Ni₆₀Al_{24.5}Fe_{15.5} ternary shape memory alloys [J]. *Journal of Alloys and Compounds*, 2013, 571: 63–68.

形状记忆合金非常规加工综述

M. MANJIAH¹, S. NARENDRANATH¹, S. BASAVARAJAPPA²

1. Department of Mechanical Engineering, National Institute of Technology, Surathkal, Karnataka, India;

2. Department of Studies in Mechanical Engineering, University B.D.T. College of Engineering,
Davangere 577004, Karnataka, India

摘要: 形状记忆合金(SMAs)由于具有多种特殊性能,如伪弹性、形状记忆效应、生物相容性、高的比强度、高耐蚀性、高耐磨性、良好的抗疲劳性能,成为不断发展的先进材料。因此,形状记忆合金被广泛应用于航空航天、医疗和汽车等方面。然而,由于严重的加工硬化和伪弹性,形状记忆合金的传统加工会造成严重的刀具磨损、费时以及低维畸变。这些材料可以使用非传统的方法,如激光加工、水射流加工(WJM)和电化学加工(ECM)进行机械加工,但这些方法受限于该材料的复杂性和力学性能。而电火花加工(EDM)和线切割(WEDM)能够很好的加工具有复杂形状和精密尺寸的形状记忆合金。介绍大量关于使用电火花和线切割加工形状记忆合金的研究,分析不同研究的差异,并展望未来的研究趋势。

关键词: 非常规加工; 电火花加工; 电火花线切割; 形状记忆合金

(Edited by Chao WANG)